

# Stability of Transparent Spherically Symmetric Thin Shells and Wormholes

Mustapha Ishak\* and Kayll Lake\*\*

*Department of Physics, Queen's University, Kingston, Ontario, Canada, K7L 3N6*

(February 7, 2008)

The stability of transparent spherically symmetric thin shells (and wormholes) to linearized spherically symmetric perturbations about static equilibrium is examined. This work generalizes and systematizes previous studies and explores the consequences of including the cosmological constant. The approach shows how the existence (or not) of a domain wall dominates the landscape of possible equilibrium configurations.

04.20.Cv, 04.20.Gz, 04.70.Bw

## I. INTRODUCTION

It is difficult to imagine a geometrical construction more fundamental than an embedded hypersurface across which the second fundamental form is discontinuous. Studies of such constructions within the Darmois [1] - Israel [2] formalism (and others) have seen widespread application in classical general relativity (e.g. [3]). The importance of such a construction is of course not limited to classical general relativity but is in a real sense central to a much wider class of considerations, such as brane world cosmologies [4].

In this paper we examine the stability of spherically symmetric thin shells, which are in a clearly defined sense “transparent”, to linearized spherically symmetric perturbations about static equilibrium under the assumption that the shells remain transparent under perturbation. The study of the stability of shells is not new [5]. Here we follow Poisson and Visser [6] and parameterize the stability of equilibrium so that we do not have to specify a surface equation of state. The present work generalizes and systematizes previous studies and shows how the existence (or not) of a domain wall [7] dominates the landscape of possible equilibrium configurations.

## II. STABILITY

### A. Equation of Motion

We use the notation of Musgrave and Lake [3] throughout and consider a 3-surface  $\Sigma$  dividing spherically symmetric spacetime into two distinct parts. In the spherically symmetric case, in terms of the intrinsic coordinates  $(\tau, \theta, \phi)$ , the metric intrinsic to  $\Sigma$  can be given as

$$ds_\Sigma^2 = R^2(\tau)d\Omega^2 + \epsilon d\tau^2 \quad (1)$$

where  $\Sigma$  is timelike (spacelike) for  $\epsilon = -1(+1)$  and  $d\Omega^2$  is the metric of a unit sphere. In terms of the surface energy density  $\sigma(\tau)$ , the surface mass of  $\Sigma$  is defined by

$$M(\tau) = 4\pi R^2 \sigma = \epsilon \gamma_{\theta\theta} \quad (2)$$

where  $\gamma_{\theta\theta} = [K_{\theta\theta}]$  and  $K_{ab}$  denotes the second fundamental form of  $\Sigma$ . (Our notation is explained in [8].) We have

$$K_{\theta\theta}^2 = R^2 \left( \dot{R}^2 - \epsilon \left( 1 - \frac{2m}{R} \right) \right) \quad (3)$$

where  $m$  (in general not a constant) is the (invariantly defined [9]) effective gravitational mass of one of the enveloping spacetimes. The identity

$$K_{\theta\theta}^{+2} = \frac{1}{4M^2} (K_{\theta\theta}^{+2} - K_{\theta\theta}^{-2} + M^2)^2 \quad (4)$$

can be written in the form [10]

$$\dot{R}^2 = \epsilon + \left( \frac{[m]}{M} \right)^2 - \frac{2\epsilon \overline{m}}{R} + \left( \frac{M}{2R} \right)^2. \quad (5)$$

We refer to (5) as “the equation of motion” for  $\Sigma$ . This is a quadratic identity and applies to both shells and wormholes.

## B. Transparency Condition

In this paper we use the transparency condition

$$[G_{\beta}^{\alpha} n_{\alpha} u^{\beta}] = 0, \quad (6)$$

where  $G_{\beta}^{\alpha}$  is the (4-dimensional) Einstein tensor,  $u^{\alpha}$  is the 4-tangent to  $\Sigma$  and  $n^{\alpha}$  the 4-normal to  $\Sigma$ . It follows from (6) that for  $\sigma' \neq 0$

$$\left(\frac{M}{2R}\right)'' = \frac{\Upsilon}{2R^3} \left(1 + 2\frac{P'}{\sigma'}\right) \quad (7)$$

where

$$\Upsilon \equiv 3M - (MR)' = 8\pi R^2(\sigma + P), \quad (8)$$

$' \equiv \frac{d}{dR}$  and  $P$  denotes the intrinsic surface pressure.

## C. Restrictions from the Potential

In (5)  $m$  is defined in terms of coordinates extrinsic to  $\Sigma$ . In order to view (5) as defining the potential  $V(R)$ , where

$$\dot{R}^2 = -V(R), \quad (9)$$

$R$  must define  $m$  uniquely. This imposes a restriction on the enveloping spacetimes. Consider, for example, Bondi coordinates:

$$ds^2 = 2c(v, r)dvdr - c^2(v, r)\left(1 - \frac{2m(v, r)}{r}\right)dv^2 + r^2d\Omega^2. \quad (10)$$

The continuity of the intrinsic metric gives

$$r^+ = r^- = R \quad (11)$$

so that for (9) to hold at equilibrium we require

$$m = m(r) = m(R) \quad (12)$$

which, we note, is precisely the condition that guarantees (6) at equilibrium. For (6) to hold away from equilibrium it follows that  $\frac{\partial c}{\partial r} = 0$ . In the remainder of this work we assume (12) and  $\frac{\partial c}{\partial r} = 0$  so that the shells remain transparent under perturbation. For timelike  $\Sigma$  then our assumptions require static embeddings in the neighborhood of  $\Sigma$ .

## D. $\Upsilon = 0$

In this paper we consider linearized spherically symmetric perturbations about static equilibrium. Following Poisson and Visser [6], we use  $\frac{P'}{\sigma'}(R)$  as a parameterization of the stability of equilibrium so that we do not have to specify an equation of state on  $\Sigma$ . This parameterization singles out the case  $\Upsilon = 0$ , equivalently

$$(MR)' = 3M, \quad \left(\frac{M}{2R}\right)'' = 0, \quad \sigma = -P, \quad (13)$$

where  $\sigma' = 0$ . This case (a “domain wall” [7]) signals a fundamental change in the surfaces that distinguish stable equilibria parameterized by  $\frac{P'}{\sigma'}(R)$  as it enters as an asymptote ( $\frac{P'}{\sigma'} \rightarrow \pm\infty$ ). Whereas this limit has well known concrete manifestations, for example Casimir and false vacua (*e.g.* [6]), it circumvents the usual phenomenology of  $\Sigma$  (*e.g.* [3]) since the surface stress-energy tensor of  $\Sigma$  is simply proportional to the metric intrinsic to  $\Sigma$ . In what follows we consider  $\Upsilon \neq 0$ . Whether or not this asymptote enters into a given configuration depends simply on the nature of the roots to the polynomial  $\sigma + P = 0$ . Phenomenologically, for timelike  $\Sigma$ ,  $\frac{P'}{\sigma'}(R)$  represents the square of the speed of sound on  $\Sigma$  and so one would normally expect  $0 \leq \frac{P'}{\sigma'}(R) < 1$ . However, one could also construct  $\Sigma$  out of (say) fields for which  $\frac{P'}{\sigma'}(R)$  need not even be positive. Since we are concerned with stability, not phenomenology, the plots we give generally extend beyond  $0 \leq \frac{P'}{\sigma'}(R) < 1$ .

### E. Equilibrium

From (5) and (9) it follows that the equilibrium condition  $V' = 0$  is

$$\left(\frac{M}{2R}\right)' = \frac{2R}{M} \left\{ \epsilon \left(\frac{\bar{m}}{R}\right)' - \frac{[m]}{M} \left(\frac{[m]}{M}\right)' \right\} \equiv \Gamma, \quad (14)$$

and the stability condition  $V'' > 0$  is

$$\frac{M}{2R} \left(\frac{M}{2R}\right)'' < \Psi - \Gamma^2, \quad (15)$$

where

$$\Psi \equiv \epsilon \left(\frac{\bar{m}}{R}\right)'' - \frac{[m]}{M} \left(\frac{[m]}{M}\right)'' - \left(\frac{[m]}{M}\right)'^2. \quad (16)$$

With the aide of the transparency condition (7) then the conditions for stable equilibria are

$$1 + 2\frac{P'}{\sigma} < \Phi, \quad M\Upsilon > 0, \quad (17)$$

and

$$1 + 2\frac{P'}{\sigma} > \Phi, \quad M\Upsilon < 0, \quad (18)$$

where

$$\Phi \equiv \frac{4R^4}{M\Upsilon} (\Psi - \Gamma^2). \quad (19)$$

It is perhaps worthy of note that not only is there no need for the specification of an equation of state on  $\Sigma$ , it is not necessary to even calculate  $P$ . It is only necessary to calculate  $P$  for a background check on the existence of the asymptote  $\Upsilon = 0$  by way of a search for allowed roots to the polynomial  $\sigma + P = 0$ .

### III. EXAMPLES

In the following examples the explicit form of  $\Phi$  can become lengthy. We find it instructive to demonstrate the possible equilibrium configurations graphically. In the approach we have used, the appearance (or not) of the asymptote  $\Upsilon = 0$  dominates the landscape of possible equilibrium configurations. The polynomial  $\sigma + P = 0$  is given in Appendix A.

#### A. Schwarzschild wormholes

Poisson and Visser [6] have considered the stability of Schwarzschild wormholes ( $\gamma_{\theta\theta} = 2K_{\theta\theta}^+$ ). In our notation they consider the case

$$\bar{m} = m, \quad [m] = 0, \quad \epsilon = -1, \quad M = -2R\sqrt{1 - 2\frac{m}{R}} \quad (20)$$

where  $m$  is a constant. It follows that  $\Phi$  takes a particularly simple form:

$$\Phi = \frac{m(3m - 2R)}{(R - 2m)(R - 3m)}. \quad (21)$$

Equations (17), (18) and (21) reproduce their calculation. Physical units associated with this case are given in Appendix B. The situation is generalized in Figure 1 where we have not assumed the continuity of  $m$ . For this example  $M < 0$  and  $M\Upsilon = 4R(R - 3m)$  so that the region *above* the surface (a) and *below* the surface (b) in Figure 1 correspond to stable equilibrium.

## B. Schwarzschild black holes

Brady, Louko and Poisson [11] have considered the stability of a shell surrounding a classical Schwarzschild black hole and have shown that stability conditions supersede the energy conditions for this configuration as considered previously by Frauendiener, Hoenselaers and Konrad [12]. In this case

$$m^+ > m^-, \quad \epsilon = -1, \quad M = R\sqrt{1 - 2\frac{m^-}{R}} - R\sqrt{1 - 2\frac{m^+}{R}} \quad (22)$$

where we have labelled “+” *exterior* to the shell in the sense that the event horizon is in “−”. Since  $M$  and  $\Upsilon$  are  $> 0$  it follows that the region *below* the surface shown in Figure 2 corresponds to stable equilibrium. We find that  $\frac{R}{m^+} \sim 2.37$  as  $m^- \rightarrow 0$  and that  $\frac{R}{m^+} \sim 3$  as  $m^- \rightarrow m^+$  so that  $R > 3m^-$  in agreement with previous results. There is no asymptote  $\Upsilon = 0$  in this case.

## C. Cosmological Constant

In what follows we explore the physical consequences of including a cosmological constant ( $\Lambda$ ) in the background. The only spacetimes we consider here are the Schwarzschild -de Sitter and Schwarzschild - anti de Sitter spaces so that the effective gravitational mass  $m(r)$  is given by

$$m(r) = \mathfrak{m} + \frac{\Lambda r^3}{6}, \quad (23)$$

where  $\mathfrak{m}$  is a constant.

### 1. Schwarzschild -de Sitter | Schwarzschild

Qualitatively, the inclusion of a positive cosmological constant inside a timelike shell should weaken the binding of the shell in the sense that  $P$  will become negative (a surface *tension*) to stabilize the shell at sufficiently large  $R$ . The result is quite unlike the case  $\Lambda = 0$  (above) where surface tensions are not required to stabilize the shell at any radius. This effect is demonstrated in Figure 3. In this case

$$m^+ > \mathfrak{m}^-, \quad \epsilon = -1, \quad M = R\sqrt{1 - 2\frac{\mathfrak{m}^-}{R} - \frac{\Lambda R^2}{3}} - R\sqrt{1 - 2\frac{m^+}{R}} \quad (24)$$

where again we have labelled “+” *exterior* to the shell in the sense that the innermost event horizon is in “−”. Since  $M$  and  $\Upsilon$  are  $> 0$  in this case, it follows that the region *below* the surface shown in Figure 3 corresponds to stable equilibrium. There is no asymptote  $\Upsilon = 0$  in this case.

### 2. Schwarzschild - anti de Sitter | Schwarzschild

This case is the same as the previous one except that  $\Lambda < 0$ . Qualitatively, the inclusion of a negative cosmological constant inside a timelike shell should not *require* a surface tension to stabilize the shell at sufficiently large  $R$ . Whereas this agrees with what we find (see Figure 4), in this case we find an asymptote  $\Upsilon = 0$  with the consequence that the stability surfaces resemble the wormhole case. However, since  $M > 0$  here, the regions of stability are the reverse of those for wormholes in agreement with our intuition.

### 3. Inversions of 1 and 2

By the inversion of 1 we mean

$$\mathfrak{m}^+ > m^-, \quad \epsilon = -1, \quad M = R\sqrt{1 - 2\frac{m^-}{R}} - R\sqrt{1 - 2\frac{\mathfrak{m}^+}{R} - \frac{\Lambda R^2}{3}} \quad (25)$$

with  $\Lambda > 0$  and where again we have labelled “+” *exterior* to the shell in the sense that the innermost event horizon is in “−”. In this case we find that the stability regions are qualitatively similar to Figure 4. The inverse of 2 is the same situation with  $\Lambda < 0$  and in this case we find that the stability regions are qualitatively similar to Figure 3 in agreement with intuition.

One would not expect that the inclusion of  $\Lambda$  *continuous* across  $\Sigma$  would change, in a significant way, possible equilibrium configurations. To test this consider

$$\mathfrak{m}^+ > \mathfrak{m}^-, \quad \epsilon = -1, \quad M = R\sqrt{1 - 2\frac{\mathfrak{m}^-}{R} - \frac{\Lambda R^2}{3}} - R\sqrt{1 - 2\frac{\mathfrak{m}^+}{R} - \frac{\Lambda R^2}{3}} \quad (26)$$

where again we have labelled “+” *exterior* to the shell in the sense that the innermost event horizon is in “-”. Our findings are summarized in Figure 5 which, when compared to Figure 2, agrees with what we would expect.

#### IV. CONCLUSIONS

In this paper we have examined the stability of transparent spherically symmetric thin shells to linearized spherically symmetric perturbations about static equilibrium under the assumption that the shells remain transparent under perturbation. Our approach has followed that due to Poisson and Visser [6] wherein  $\frac{P'}{\sigma}(R)$  is used as a parameterization of the stability of equilibrium. An equation of state on  $\Sigma$  is not specified. The present work generalizes and systematizes previous studies. We have found that the single feature which dominates the landscape of equilibrium configurations is the appearance or not of the asymptote  $\Upsilon = 0$ . The cosmological constant has been included in our calculations with results in agreement with intuition. We find that the closest radius for a stable shell is  $R = 3\mathfrak{m}^-$  irrespective of  $\Lambda$  and at that radius  $\frac{P'}{\sigma} = 1$ .

#### ACKNOWLEDGMENTS

This work was supported by a grant (to KL) from the Natural Sciences and Engineering Research Council of Canada and by an Ontario Graduate Scholarship (to MI). Portions of this work were made possible by use of *GRTensorII* [13].

---

\* Electronic Address: ishak@astro.queensu.ca

\*\* Electronic Address: lake@astro.queensu.ca

- [1] G. Darmon, Memorial de Sciences Mathematiques, Fascicule XXV ch V (1927).
- [2] W. Israel, Nuovo Cimento **44B** 1 (1966) and **48B** 463 (1966).
- [3] P. Musgrave and K. Lake, Class. Quantum Grav. **13**, 1885 (1996) (gr-qc/9510052).
- [4] Indeed, a simple search on “domain AND wall” in “astro-ph + gr-qc + hep-th” at [arXiv.org](https://arxiv.org) returns over 100 results for the “Last year” and over 500 results over “All years”.
- [5] For an overview of early studies on the gravitational stability of fluid shells see J. E. Chase, Nuovo Cimento **67B** 136 (1970).
- [6] E. Poisson and M. Visser, Phys. Rev. D **52** 7318 (1995) (gr-qc/9506083).
- [7] By “domain wall” here we mean a hypersurface with an intrinsic equation of state of the form  $\sigma + P = 0$ , where  $\sigma$  is the surface density and  $P$  is the surface pressure. See *e.g.* [3].
- [8] We write  $[X] \equiv X^+|_{\Sigma} - X^-|_{\Sigma}$  and  $\bar{X} \equiv (X^+|_{\Sigma} + X^-|_{\Sigma})/2$  with  $X^{\pm}|_{\Sigma}$  denoting the limiting values of  $X$  on  $\Sigma$ , and use geometrical units except in Appendix B. We use the letter “m” as follows:  $M$  is the surface mass of  $\Sigma$  defined by (2),  $m$  is the effective gravitational mass of the enveloping spacetimes “+” and “-” (see [9] and (10)),  $[m] \equiv m^+ - m^-$  and  $\bar{m} \equiv (m^+ + m^-)/2$ .  $\mathfrak{m}$  is not the effective gravitational mass but is related to it for the cases considered here by (23).
- [9] See, for example, S. Hayward, Phys. Rev. D **53** 1938 (1996) (gr-qc/9408002) and E. Poisson and W. Israel, Phys. Rev. D **41**, 1796 (1990).
- [10] K. Lake, Phys. Rev. D **19**, 2847 (1979).
- [11] P. R. Brady, J. Louko and E. Poisson, Phys. Rev. D **44** 1891 (1991).
- [12] J. Frauendiener, C. Hoenselaers and W. Konrad, Class. Quantum Grav. **7**, 585 (1990).
- [13] This is a package which runs within Maple. It is entirely distinct from packages distributed with Maple and must be obtained independently. The GRTensorII software and documentation is distributed freely on the World-Wide-Web from the address <http://grtensor.org>

## Appendix A: The Asymptote $\Upsilon = 0$

The existence of the asymptote  $\Upsilon = 0$  depends on the existence of allowed roots to the equation  $\sigma + P = 0$ . Writing

$$\mathbf{f}(R) \equiv 1 - \frac{2m(R)}{R} \quad (27)$$

these roots are determined by the polynomial

$$\delta\sqrt{F}(2f - Rf') = \sqrt{f}(2F - RF') \quad (28)$$

where  $\delta = +1$  for shells,  $\delta = -1$  for wormholes and we have distinguished the sides of  $\Sigma$  by  $\mathbf{f} = f$  and  $\mathbf{f} = F$ . As an example, the solution to equation (8) for the Schwarzschild wormhole case (see Figure 1) is shown in Figure 6.

## Appendix B: Physical Units and Schwarzschild wormholes

R(km)	$R/M$	$M/M_\odot$	$(P'/\sigma')_{min}$		R(km)	$R/M$	$M/M_\odot$	$(P'/\sigma')_{max}$
1	-1.0	-0.67721	4.75		1	-0.55	-1.23130	-0.62
1	-1.5	-0.45148	3.50		1	-0.60	-1.12869	-0.81
1	-2.0	-0.33861	4.98		1	-0.65	-1.04187	-1.12
1	-2.5	-0.27089	7.14		1	-0.70	-0.96745	-1.64
1	-3.0	-0.22574	9.84		1	-0.75	-0.90295	-2.69
1	-10.0	-0.06772	100.76		1	-0.85	-0.79672	-25.80
5	-1.0	-3.38607	4.75		5	-0.55	-6.15648	-0.62
5	-1.5	-2.25738	3.50		5	-0.60	-5.64344	-0.81
5	-2.0	-1.69303	4.98		5	-0.65	-5.20933	-1.12
5	-2.5	-1.35443	7.14		5	-0.70	-4.83724	-1.64
5	-3.0	-1.12869	9.84		5	-0.75	-4.51475	-2.69
5	-10.0	-0.33861	100.76		5	-0.85	-3.98361	-25.80
10	-1.0	-6.77213	4.75		10	-0.55	-12.31297	-0.62
10	-1.5	-4.51475	3.50		10	-0.60	-11.28689	-0.81
10	-2.0	-3.38607	4.98		10	-0.65	-10.41866	-1.12
10	-2.5	-2.70885	7.14		10	-0.70	-9.67447	-1.64
10	-3.0	-2.25738	9.84		10	-0.75	-9.02951	-2.69
10	-10.0	-0.67721	100.76		10	-0.85	-7.96721	-25.80
100	-1.0	-67.72131	4.75		100	-0.55	-123.12966	-0.62
100	-1.5	-45.14754	3.50		100	-0.60	-112.86886	-0.81
100	-2.0	-33.86066	4.98		100	-0.65	-104.18664	-1.12
100	-2.5	-27.08853	7.14		100	-0.70	-96.74473	-1.64
100	-3.0	-22.57377	9.84		100	-0.75	-90.29508	-2.69
100	-10.0	-6.77213	100.76		100	-0.85	-79.67213	-25.80

TABLE I. Physical units associated with the wormhole case with continuous mass. Values for the upper branch in Figure 7 are shown on the left.

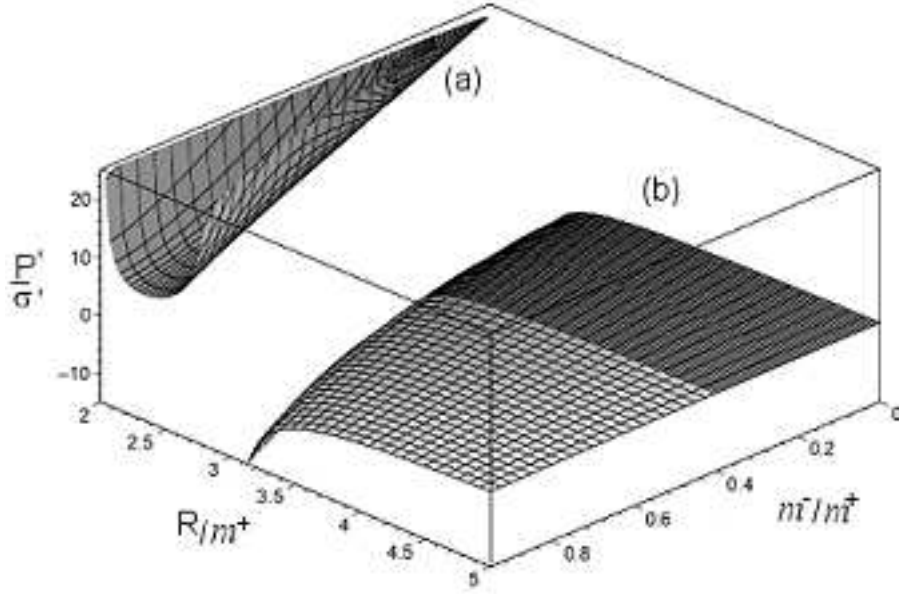


FIG. 1. A generalization of the work by Poisson and Visser in which  $m$  is not assumed continuous across  $\Sigma$ . The region *above* the surface (a) and *below* the surface (b) correspond to stable equilibrium. The figure given by Poisson and Visser is the slice  $m^- = m^+$ . The position of the asymptote  $\Upsilon = 0$  for this case is shown in Figure 6.



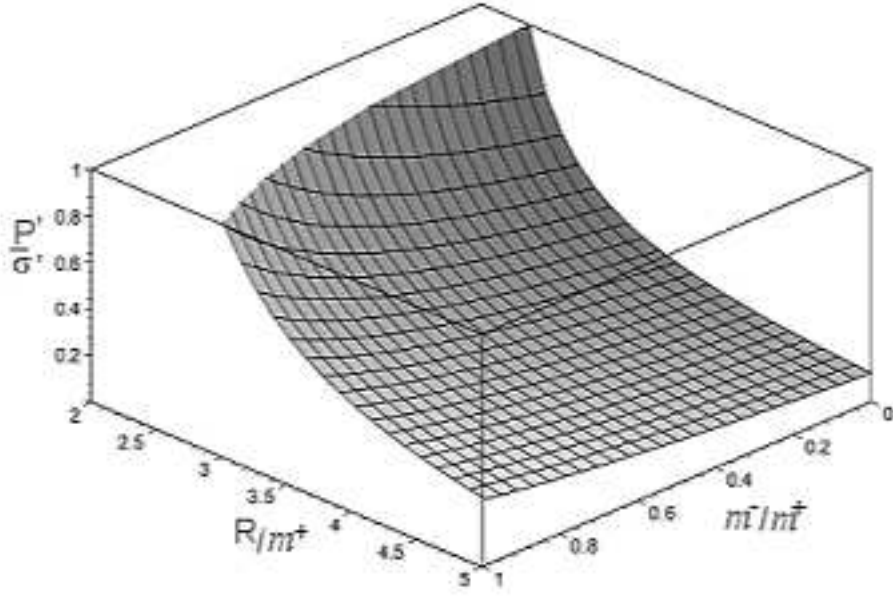


FIG. 2. A reproduction of the classical Schwarzschild black hole case examined by Brady, Louko and Poisson. Since  $M$  and  $\Upsilon > 0$  it follows that the region *below* the surface shown corresponds to stable equilibrium. For  $\frac{P'}{\sigma} = 1$  we find that  $\frac{R}{m^+} \sim 2.37$  as  $m^- \rightarrow 0$  and that  $\frac{R}{m^+} \sim 3$  as  $m^- \rightarrow m^+$  so that  $R > 3m^-$  in agreement with previous results.

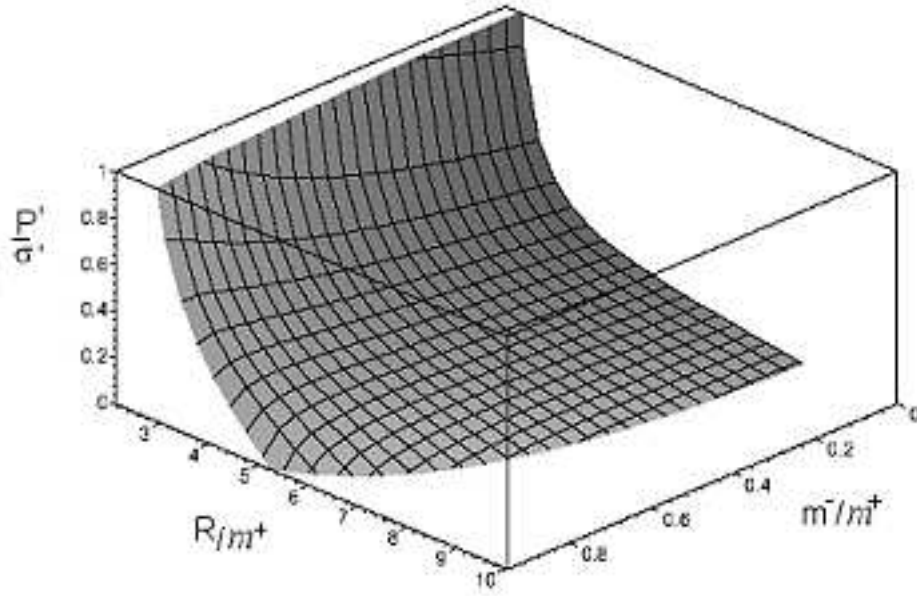


FIG. 3. Schwarzschild - de Sitter black hole in a Schwarzschild background. Since  $M$  and  $\Upsilon$  are  $> 0$  in this case, it follows that the region *below* the surface shown corresponds to stable equilibrium. The inclusion of a positive cosmological constant inside a timelike shell weakens the binding of the shell in the sense that  $P$  becomes negative (a surface *tension*) to stabilize the shell at sufficiently large  $R$ . The result is quite unlike the case  $\Lambda = 0$  where surface tensions are not required to stabilize the shell at any radius. Here  $\Lambda m^{+2} \sim 10^{-3}$  well away from degeneracy in all cases.

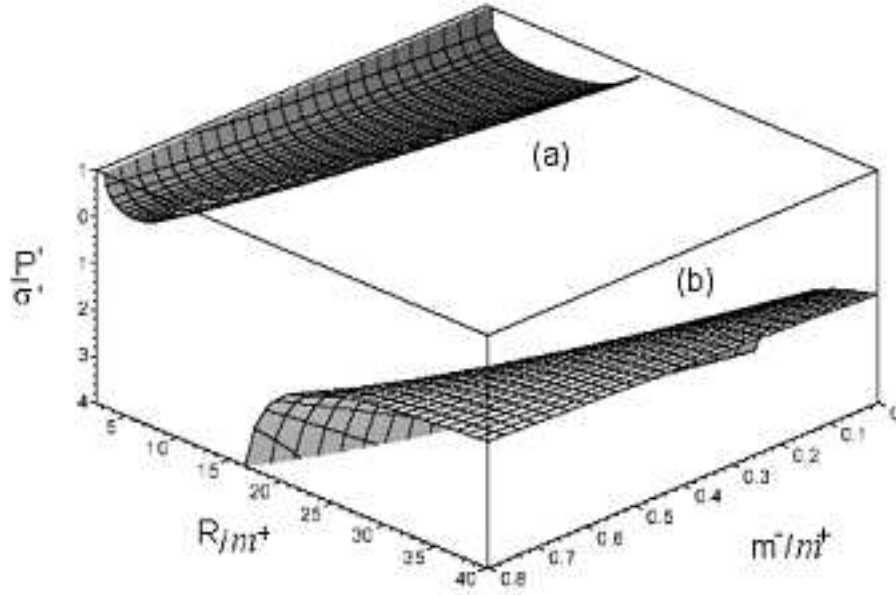


FIG. 4. Schwarzschild -anti de Sitter black hole in a Schwarzschild background. This case is the same as Figure 3 except that  $\Lambda < 0$ . Unlike the previous case however, we do find an asymptote  $\Upsilon = 0$ . Since  $M > 0$ , it follows from the form of  $\Upsilon$  that the region *below* (a) and *above* (b) are the regions of stability. Here again  $\Lambda m^{+2} \sim 10^{-3}$  well away from degeneracy in all cases.

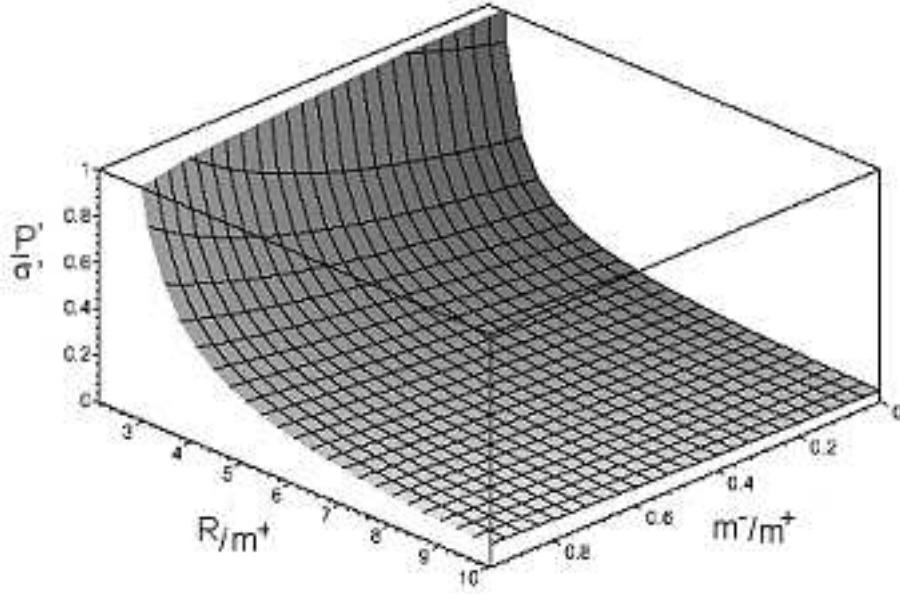


FIG. 5. Schwarzschild - de Sitter black hole in a Schwarzschild - de Sitter background with  $[\Lambda] = 0$ . In this case one would expect that  $\Lambda$  would not change the qualitative features of equilibrium. This is exactly what we find (see Figure 2). Here  $\Lambda m^{+2} \sim 10^{-3}$  well away from degeneracy in all cases. The diagram remains qualitatively unchanged under a change in the sign of  $\Lambda$  as long as  $[\Lambda] = 0$ .

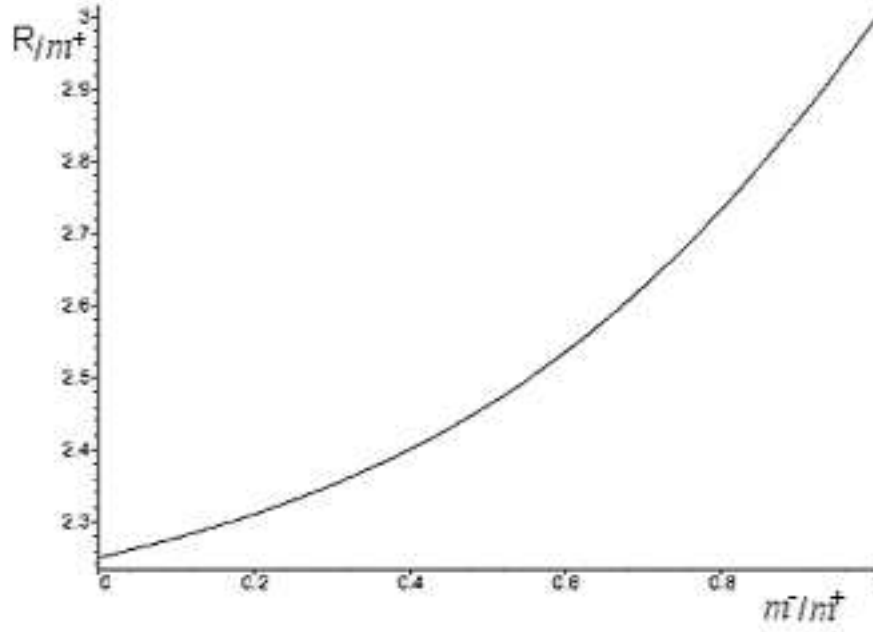


FIG. 6. The asymptote  $\Upsilon = 0$  for the Schwarzschild wormhole (see Figure 1). The plot shows the allowed roots to equation (8).

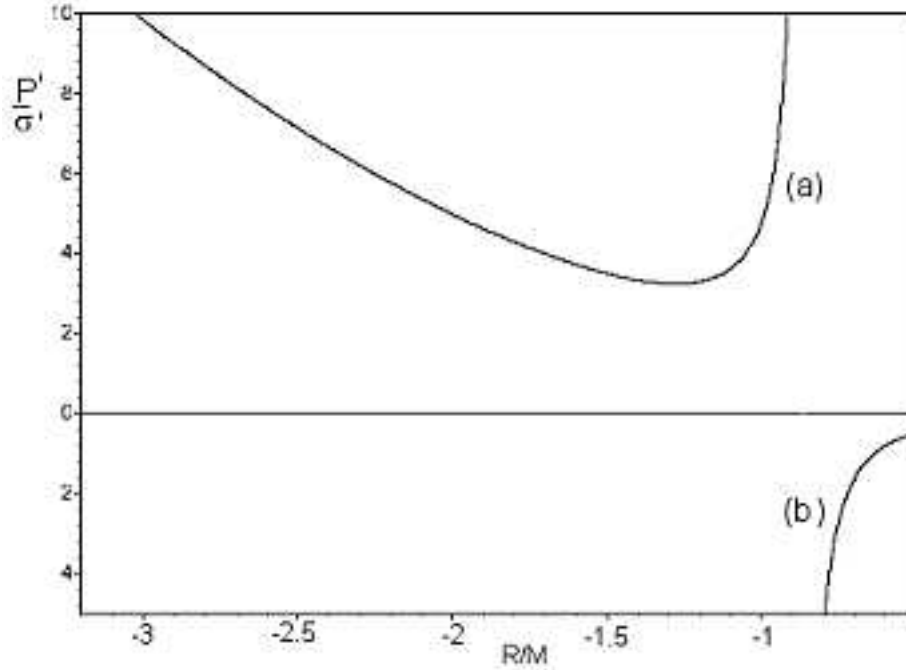


FIG. 7. Plot of stability regions versus  $R/M$  ( $M$  is the intrinsic mass) for the case considered by Poisson and Visser . The region *above* the curve (a) and *below* the curve (b) correspond to stable equilibrium. The position of the asymptote  $\Upsilon = 0$  is at  $R/M = -\sqrt{3}/2$  corresponding to  $R/m = 3$ .